Electronic Supplementary Material (ESI) for RSC Advances.
This journal is © The Royal Society of Chemistry 2015

Supplementary Information

Structure and Electrical Properties of Tetragonal Tungsten Bronze $Ba_2CeFeNb_4O_{15}$

Hongqiang Ma[a], Kun Lin[a], Laijun Liu[c], Baoling Yang[a], Yangchun Rong[a], Jun Chen[a] , Jinxia Deng[ab], Shogo Kawaguchi[d], Kenichi Kato[e], Xianran Xing*[,a]

[a] *Department of Physical Chemistry,* [b] *Department of Chemistry, University of Science and Technology Beijing, Beijing 100083, China*

[c] *State Key Laboratory Breeding Base of Nonferrous Metals and Specific Materials Processing, Guilin University of Technology, Giulin 541004, China*

[d]*Japan Synchrotron Radiation Research Institute (JASRI)1-1-1, Kouto, Sayo-cho, Sayo-gun, Hyogo 679-5198, Japan*

[e] *RIKEN SPring-8 CenterSayo, Hyogo 679-5148, Japan*

Corresponding author

Department of Physical Chemistry, University of Science and Technology Beijing, Beijing 100083, China

Tel: + 86-10-62334200

Fax: + 86-10-62332525

*e-mail address: xing@ustb.edu.cn

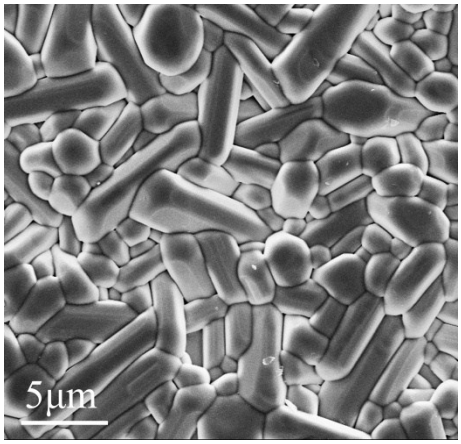

Fig. S1. SEM image of selected pellets surface for the as-synthesized BCFN.

The microstructure of BCFN ceramics was observed by scanning electron microscopy (SEM, Supra 55; Zeiss, Oberkochen, Germany). No impurity was observed.

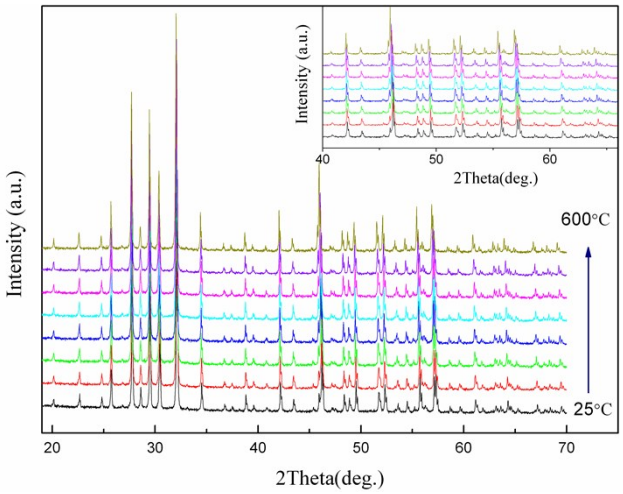

Fig. S2 XRD patterns of BCFN powder at different temperatures (25 – 600 °C). It shows that no phase transition occurs in the measured temperature.

The high-temperature powder X-ray diffraction patterns were collected on a laboratory diffractometer, (PANalytical X' Pert^{III}, Holland, Cu Kα, λ=1.5406 Å) and an Anton Par HTK 1200 high-temperature attachment was used. Data were collected in 0.0131° steps. The heating rate was 10 °C/min, and the sample was held for 15 min at a specified temperature to reach heating equilibrium.

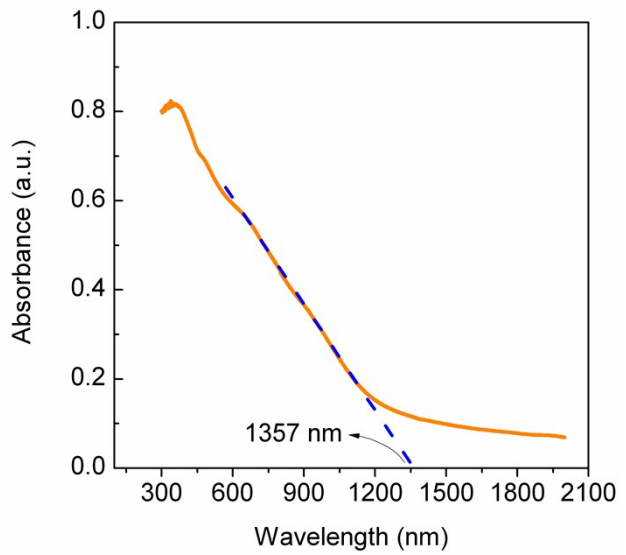

Fig. S3 UV-vis absorbance spectroscopy of as-sintered BCFN powders**.** Band gap estimated from the intercept of tangents to the plots was ~0.91 eV indicative of the existence of shallow energy levels due to oxygen vacancies.

UV-vis absorbance spectroscopy of the nanostructures was performed using a UV-vis spectrometer (VARIAN, Cary 5000) in a quartz cuvette.

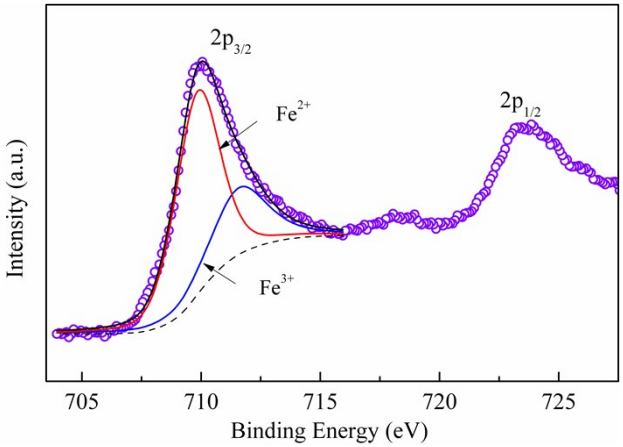

Fig. S4 X-ray photoelectron spectra of Fe2p for surface of as-sintered BCFN pellet. It suggests that the Fe^{3+} reduction to Fe^{2+} and oxygen loss in BCFN are significant in surface.

The surface properties of samples were characterized by X-ray photoelectron spectroscopy (XPS) on a ESCALAB 250 Xi (VG, UK) with Carbon (284.8 eV) as a marker.

Table S1 BVS Values Based on the Data Obtained from SPD Data

Atom	BVS	Atom	BVS
Ce	2.87(2)	O1	1.89(1)
Ba	2.02(1)	O2	2.06(2)
Fe1	3.31(3)	O3	1.95(1)
Nb1	5.10(4)	O4	2.22(3)
Fe2	3.31(3)	O5	1.98(3)
Nb2	5.10(4)		

Bond valence sums (BVS)[1] calculated from the refinements in Table S1 supports the validity of the structure and indicates the dominated existence of Fe^{3+} and Ce^{3+} instead of Fe^{2+} and Ce^{4+}. Based on the XPS data in Fig. S4, defect concentration in surface are larger than that inside the grains.

[1] D. Brown, and D. Altermatt, *Acta Crystallogr.* 1985, **B41**, 244-247.